

Article

A Study on the Results of Risk Analyses Applying the Concept of Rock Mass Stand-Up Time for Underground Mining Sites

Phong Duyen Nguyen¹ , Hiep Huy Nguyen², Hung Huu Dam³, Manh Van Nguyen¹, Piotr Osinski^{4,*} 
and Eugeniusz Koda^{4,*} 

- ¹ Department of Underground Construction and Mining, Hanoi University of Mining and Geology, Hanoi 100000, Vietnam; nguyenduyenphong@humg.edu.vn (P.D.N.); nguyenvanmanh@humg.edu.vn (M.V.N.)
- ² Internal Combustion Engine Department, Le Quy Don Technical University, Hanoi 11917, Vietnam; huyhiepnguyen@lqdtu.edu.vn
- ³ Soil Mechanics and Geotechnics Department, Moscow State University of Civil Engineering, Moscow 129337, Russia; hungdh@beavergr.ru
- ⁴ Institute of Civil Engineering, Warsaw University of Life Sciences, 02-787 Warsaw, Poland
- * Correspondence: piotr_osinski@sggw.edu.pl (P.O.); eugeniusz_koda@sggw.edu.pl (E.K.); Tel.: +48-59-35216 (P.O.); +48-59-35219 (E.K.)

Abstract: Throughout all the countries in the world, including Vietnam, nations with well-established mining industries have undertaken extensive research on the stability of rock masses when constructing underground tunnels in varied geological conditions. The present study aims to provide a comprehensive overview of the risk assessment related to rock masses during the construction of pit lines in mining operations. Consequently, the standing time of unsupported tunnels is assessed based on different values of the strength index and deformation characteristics of the rock mass. The objective was to perform both experimental and theoretical investigations to analyse how the stand-up time of rock masses surrounding a tunnel affects the unsupported span. The analyses were based on considering the rock parameters, including strain modulus; geological strength index; and allowable displacement values, and consideration of hereditary creep properties. By examining tunnels excavated in rock strata, it was concluded that varying geological strength index values resulted in distinct creep behaviour in the surrounding rock masses. Thus, it was reasonable to compute the unsupported span and stand-up time of tunnels. The research revealed that permissible displacements are significantly influenced by the types of rock materials surrounding the tunnel structure. Recognising the significance of time, the authors introduce a more practical interpretation and evaluation of the stability of rock masses, thus enhancing the precision of commonly available models.

Keywords: risk; rock mass; stand-up time; underground mines; GSI; modulus



Citation: Nguyen, P.D.; Nguyen, H.H.; Dam, H.H.; Nguyen, M.V.; Osinski, P.; Koda, E. A Study on the Results of Risk Analyses Applying the Concept of Rock Mass Stand-Up Time for Underground Mining Sites. *Appl. Sci.* **2024**, *14*, 1736. <https://doi.org/10.3390/app14051736>

Academic Editors: Mien Jao, Paul Bernazzani and Stefano Invernizzi

Received: 5 January 2024

Revised: 6 February 2024

Accepted: 16 February 2024

Published: 21 February 2024



Copyright: © 2024 by the authors. Licensee MDPI, Basel, Switzerland. This article is an open access article distributed under the terms and conditions of the Creative Commons Attribution (CC BY) license (<https://creativecommons.org/licenses/by/4.0/>).

1. Introduction

The stand-up time of the rock mass surrounding an unsupported tunnel plays a crucial role in underground construction overall, especially in the context of tunnelling. The assessment of stand-up time values carries substantial importance in the selection of efficient excavation methods and support systems. The primary aim of the study was to apply a defined set of input data that validates the impact of permissible displacement on the stand-up time of argillite stone in tunnel construction. The objective was to perform experimental and theoretical investigations to analyse the impact of stand-up time on the unsupported span of rock masses around tunnels. This analysis was based on implementing mechanical rock parameters like strain modulus, the Geological Strength Index (GSI), and allowable displacement values, and also considers hereditary creep properties. The use of a temporal dimension introduces a dynamic aspect to the calculation of stand-up time,

addressing a critical factor that has usually been neglected in available published research. By considering the time factor, the authors provide a more realistic scenario for evaluating rock mass stability, thus contributing to the enhancement of models established in the past.

The term “stand-up time” was first proposed in Lauffer’s rock mass classification [1]. The purpose of the classification was to generate the relationship between the time that it took to apply supporting systems and rock mass quality after the excavation of unsupported tunnels. The unsupported tunnel span is defined as the distance between the tunnel face and the nearest support if it is greater than the width of the cross-section of the structure. In addition, R. Hooke [2] defines stand-up time as the amount of time a tunnel is capable of withstanding stresses without any supporting systems. In other words, it is the time that a rock mass remains stable and no collapsing event is observed. The magnitude of stand-up time plays a key role in tunnelling since it significantly affects excavation works [3].

Rock masses are typically classified into different grades, which vary from A to G corresponding to the relationship between the stand-up time and the supporting structures. Thus, A stands for highly stable rock masses, and G refers to poorly stable ones. The analyses of the research outcomes proposed by Lauffer [1] confirmed that values of stand-up time decrease with an increase in unsupported tunnel spans. This proposal given by Lauffer was modified and linked to the rock masses classification suggested in several other studies. Improved classifications refer to the Q system (a concrete grade of rock quality), the RMR system, and the NATM (New Austria Tunnelling Method). Barton and Bieniawski [4] introduced a new relationship between stand-up time and maximum unsupported tunnel span (L). In addition, based on the Rock Mass Rating (RMR), [5] also proposed a method of determining average values of stand-up time corresponding to the unsupported tunnel span (L).

Stand-up time is greatly influenced by the mechanical parameters of the rock mass, which comprise a modulus of rock mass; compressive strength; in-situ stress state; water pressure; seepage; and joint systems. In addition, excavation technology, such as drilling and blasting; mechanical excavation; and the various shapes of tunnel cross sections, also greatly affect the stand-up time of rock. The authors of [6] investigated the interaction of tunnel face dimensions and excavation rates with the stand-up time. As a result, they first concluded that an increase in excavation rate, or a contraction of the tunnel cross-section, leads to an increase in stand-up time. Secondly, they pointed out that tunnelling techniques significantly impact tunnel stability. A mechanical excavation would tend to improve tunnel stability more than blasting techniques.

By considering the geometrical parameters of the considered tunnel span and the deformation characteristics of the rock mass around the tunnel, the authors of [3] established the relationship between the unsupported tunnel span (L^*) and the stand-up time (t^*), which is expressed using the formula given below,

$$L^* t^{*(1-\alpha)} = \frac{4E}{3\gamma H} \frac{(1-\alpha)}{\delta} u_l^* \quad (1)$$

where: L^* is the unsupported tunnel span according to [1]; $L^* = 2R = B$; t^* stands for the stand-up time; α is a dimensionless empirical parameter; δ is a dimensional parameter ($s - 1 + \alpha$); E is the modulus of elasticity of the rock mass; γ stands for the unit weight of the rock mass; H is the tunnel depth; and u_l^* is the allowable displacement for maintenance of the sustainable condition of sedimentary rocks (for all the parameters used in the equations, please refer to Abbreviations part).

To determine the physical and mechanical properties of a rock mass, the modulus of elasticity of rock mass is required to be determined by an empirical method of analysis, and then the formula for stand-up time is established based on the rheological properties of the rock mass. In addition, the parameters of the GSI also present a significant impact on the stability of an unsupported tunnel. As a result, the authors confirm that tunnelling techniques are greatly influenced by the values of stand-up time. However, by precisely assessing rock mass properties (GSI parameters and the modulus of elasticity), engineers

are capable of applying adequate supporting structures which are optimal for unsupported tunnel spans.

Upon tunnel excavation, the surrounding rock mass may deform gradually, resulting in a potential collapse caused by the creep properties of the rock medium [7–10]. The research on the influence of time on failure states, and the discussion on creep damage of a rock mass are broadly available in the literature [7,11–13]. A great number of investigations of rock creep behaviour indicate that portions of time-varying deformation of rock masses or rock specimens contribute to the development of total displacements [14–19]. The time dependence of rock mechanical behaviour leads to gradual deformation. Therefore, tunnel structure stability calculation and design demand the precise determination of the rheological properties of surrounding rock mediums, to provide safe conditions during excavation works [14,15].

Figure 1 presents a typical rheological curve, which comprises four basic stages when a specimen is compressed by a constant axial load [7,15,20,21]. All the stages are represented as follows:

- The first stage describes the elastic loading; the instantaneous deformation is observed as reversible.
- The second stage shows the primary creep, in which the deformation increases nonlinearly.
- The third stage denotes the secondary creep process, where the deformation grows steadily and nearly linearly.
- The fourth stage is characterised by an explicit curve of irreversible deformation with the acceleration of creep rate. This stage ends up in the entire failure of tested specimens.

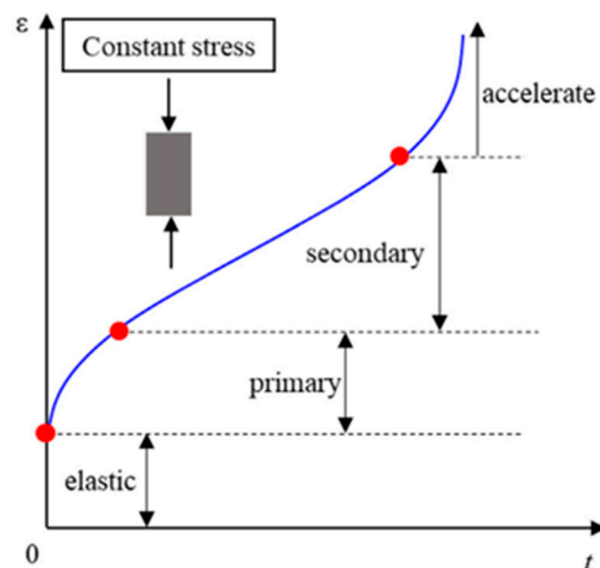


Figure 1. Creep response—a conceptual model of rheological curve.

In rock mechanics, creep is defined as the convergence of shear strain with constant volumetric strain under the maintenance of an unchanging load. When being loaded, a specimen experiences instantaneous deformations which can be mathematically described using Hooke's laws [2]. During a test, it is observed that the cumulative irreversible deformation of a specimen increases with a decrease in the deformation rate. In the case of being constantly loaded, the specimen's deformation and time function is nearly linear. Afterwards, the stage of the test specimen can remain in the secondary creep state or turn into the failure stage. Theoretically, volumetric strains remain constant during the creep process. However, this assumption is only considered reasonable when deviatoric strains stem from realistic deformation due to diffusion or displacement of solids [22–25]. The creep of various materials, such as salt rocks, steel, and other ductile materials, are mostly

observed in a relatively short time. Nevertheless, it is possible to observe the creep effect in hard rocks and brittle rocks under appropriate conditions over a long period.

In underground tunnels, creep processes are generally observed together with the contraction of the tunnel section diameter with time [15,26]. This behaviour can be considered a compression and swelling phenomenon of weak and soft rocks [27,28]. Swelling is defined as the volume change of rocks containing clay particles, such as montmorillonite and other components, with high swelling capacity [29].

The proposed study aims to advance existing knowledge by incorporating hereditary creep properties into the calculations of tunnel construction stability. This research introduces a dynamic element to the estimation of stand-up time, addressing a crucial aspect that has been overlooked in available scientific publications. Analyses of the influence of time would allow a better understanding of the mechanisms to assure a more detailed assessment and interpretation of rock mass stability, thereby contributing to the refinement of existing models. Performed analyses and computations allow the integration of time-dependent factors, providing a more accurate understanding of the stand-up time for rock masses around unsupported tunnels. The present research aims to contribute to the optimisation of underground construction practices, serving as a valuable resource for engineers and practitioners through modelling and experimental investigation.

2. Materials and Methods

Considering one of the hereditary creep theories, presented in [30,31], the authors took into account the nonlinear properties of the material and compared these with the time taken. The creep theory was also applied in slope stability-related research, showing a broad approach of numerical and empirical application [32]. Hereditary creep allows for the manifesting of material deformation over a long period, taking into consideration the history of the loading processes. According to hereditary creep theory, materials continue deforming after being loaded and unloaded. The strains are proportional to the stress values at various intervals and accumulate gradually. The equation to present the relationship of nonlinear strain and stress, taking into account the time factor according to Volterra's hereditary creep theory [30], is shown as follows:

$$\varepsilon(t) = \frac{1}{E} \left[\sigma(t) + \int_0^t L(t, \tau) \cdot \sigma(\tau) d\tau \right] \quad (2)$$

where $\varepsilon(t)$, $\sigma(t)$ are the strain and stress at moment t , respectively; E stands for the instantaneous modulus of the elasticity of rocks; τ is the time before instant t ; and $L(t, \tau)$ is a creep kernel function characterising the strain rate.

Based on the hereditary properties of rock, the creep kernel $L(t, \tau)$ can be presented as follows:

$$L(t, \tau) = \delta(t - \tau)^{-\alpha} \quad (3)$$

The strain archived from the creep test for a rock specimen by loading with a constant load, $\sigma = \sigma_0 = \text{const}$ obeys the law as follows:

$$\varepsilon(t) = \frac{\sigma_0}{E_0} (1 + \Phi) \quad (4)$$

Nowadays, there are various laboratory methods to determine the creep parameters of rock specimens. One of them is the bending compression test performed on rock specimens with a beam of a cross-section of $20 \times 20 \times 160$ mm; the testing scheme is represented in Figure 2. The laboratory tests were performed using the creep apparatus comprised of a stainless-steel test cylinder sealed at both ends and equipped with externally linked pistons. By ensuring that the pistons share the same diameter, this setup facilitated the deformation of the specimen without altering the volume in the pressure chamber. The axial load or differential stress on the specimen was applied via an overhanging pan atop the yoke of the

apparatus, loaded with the desired weights. The contraction of the specimen was gauged using an Ames dial gauge affixed to the upper-end piece of the specimen assembly.

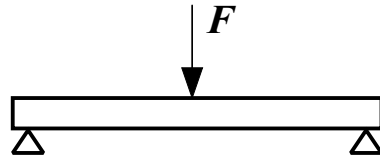


Figure 2. Scheme of bending and compressing test of a rock specimen.

In accordance with [3], creep function Φ is expressed as follows:

$$\Phi = \frac{\delta \cdot t^{1-\alpha}}{1-\alpha} \tag{5}$$

where Φ is the creep function; σ_0 is tensile stress due to the bending moment, MPa; E is the strain modulus of rock, and GPa; α and δ are dimensionless and dimensional empirical parameters, respectively.

Taking into consideration Equation (4) the time-varying deformation modulus can be expressed as:

$$E_t = \frac{E}{1+\Phi} \tag{6}$$

The deflection of the rock beam was determined using the following formula,

$$y = \frac{F \cdot l^3}{48 \cdot E \cdot J} \tag{7}$$

where: J is the moment of inertia of the beam cross-section.

The tensile stress arising from bending the rock beam was calculated using the following formula,

$$\sigma = \frac{M \cdot h}{2J} \tag{8}$$

where: M is the maximum bending moment at the centre beam cross-section, and h is the beam height.

$$M = \frac{F \cdot l}{4} \tag{9}$$

Combining (8), (9) and (7) the formula could be presented as follows:

$$y = \sigma \cdot \frac{l^2}{6E \cdot h} \tag{10}$$

Substituting E by E_t in Equation (10), taking into consideration Equation (6) the formula for calculating the beam deflection at the centre cross-section with time can be expressed as follows:

$$y(t) = \sigma \frac{l^2}{6E \cdot h} (1 + \Phi) \tag{11}$$

The initial instantaneous beam deflection obtains the values of:

$$y_0 = \sigma \frac{l^2}{6E \cdot h} \tag{12}$$

The Equation (11) is now:

$$y(t) = y_0 \left(1 + \frac{\delta}{1-\alpha} t^{1-\alpha} \right) \tag{13}$$

Taking logarithms of both sides of the achieved expression above, the formula is as follows:

$$\lg\left(\frac{y(t)}{y_0} - 1\right) = \lg\left(\frac{\delta}{1 - \alpha}\right) + (1 - \alpha)\lg t \tag{14}$$

Setting the following terms,

$$u = \lg\left(\frac{y(t)}{y_0} - 1\right); x = \lg t; a = \lg\left(\frac{\delta}{1 - \alpha}\right); b = 1 - \alpha \tag{15}$$

Expression (14) transforms into the first-degree equation of

$$u = a + bx \tag{16}$$

Creep parameters expressed in Equation (15) can be determined using the following formulas,

$$\alpha = 1 - b \tag{17}$$

$$\delta = 10^a(1 - \alpha) \tag{18}$$

The rock beam testing performed according to the scheme presented in Figure 2 was considered at various values of concentrated load generating the following values of tensile stress: $\sigma = 1.8; 2.25; 2.7$ (MPa). The results representing the measured displacements are given in Figure 3.

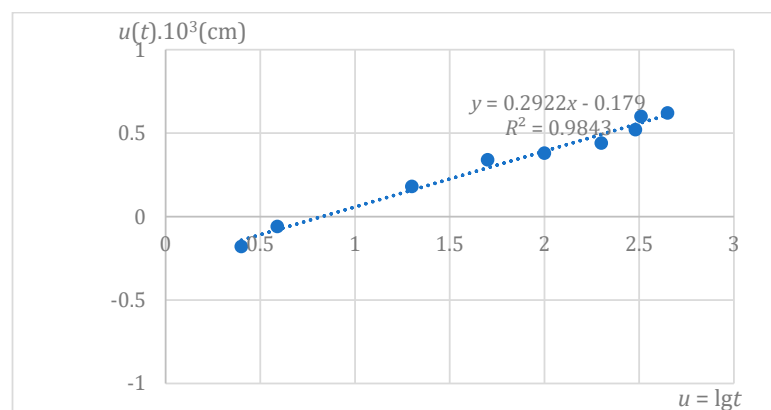


Figure 3. Result of processed output data using Equation (16).

From the results, the values of a and b were respectively equal to -0.18 and 0.29 , thereby creep parameters α and δ were calculated as follows:

$$\alpha = 1 - b = 1 - 0.29 = 0.71$$

$$\delta = 10^a(1 - \alpha) = 10^{-0.18}(1 - 0.71) = 0.192$$

Substituting α and δ achieved above into expression (5), a new form of creep function Φ can be proposed:

$$\Phi = \frac{\delta \cdot t^{1-\alpha}}{1 - \alpha} = \frac{0.192}{1 - 0.71} t^{1-0.71} = 0.662t^{0.29}$$

The initial instantaneous beam deflection y_0 was equal to 0.003 cm, corresponding to the value of tensile stress σ developing in the rock beam at 2.7 MPa. As a result, the initial instantaneous modulus of deformation of the rock beam was determined as follows:

$$y = \sigma \cdot \frac{l^2}{6E \cdot h} <-> 0.003 = 2.7 \frac{14^2}{6E \cdot 2}$$

We attain $E = 14,700$ MPa. Substituting the obtained results in Equation (13) we obtain

$$y(t) = y_0 \left(1 + \frac{\delta}{1-\alpha} t^{1-\alpha} \right) = y_0 (1 + \Phi) = y_0 (1 + 0.662t^{0.29}) \quad (19)$$

Comparison of results from Equation (19) with the experimental retrieved results at different values of tensile stress was demonstrated in the form of curves expressing creep rock beam deflection and time relationship, as presented in Figure 4.

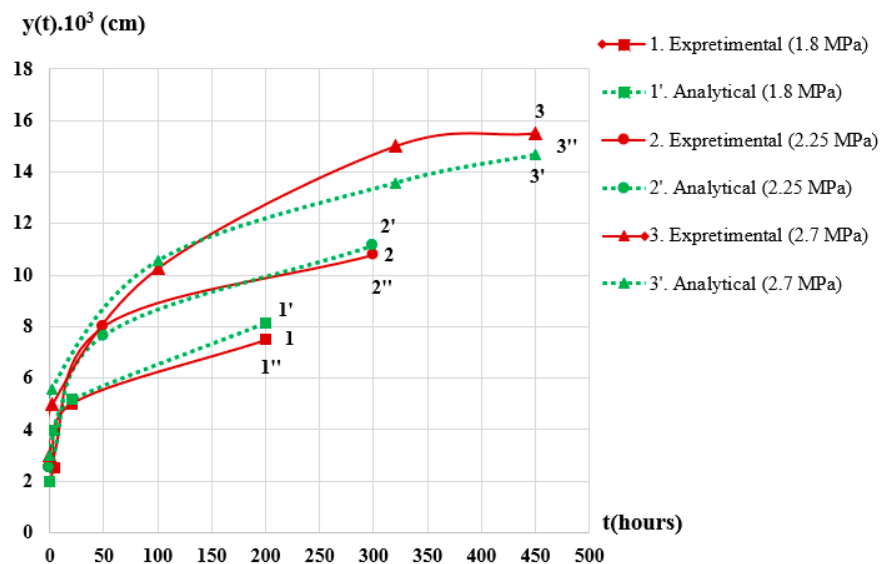


Figure 4. Relationship between rheological deformation and time, obtained by experimental and analytical approaches.

The strain modulus of rock masses is considered essential input data in the analyses of rock mass behaviours [33]. It is possible to estimate it by carrying out field tests [34], or by referring to experimental relationships obtained from tables of rock quality classification as mentioned in [35,36] (Rock Mass Rating); by [37] (Q—System); and by [38] (Geological Strength Index—GSI). Due to the time consuming and sophisticated characteristics of conducting field tests as reported by [39], the values were determined qualitatively based on classification schemes presented by [34–40].

To simplify rock classification procedures [41], a new method named GSI was proposed which concerns the input data to design underground construction in rock material. The sole system that is relevant to technical parameters, such as Mohr–Coulomb, Hoek–Brown strength parameters, or rock mass modulus, are expressed as the GSI, in accordance with [42].

The authors of [43,44] provided a quantitative base to evaluate the GSI system using proposed ratings of rock mass structure and surface condition (SCR), and a structure rating (SR) based on the volumetric joint count (J_v), and the roughness, weathering, and infilling nature of joints.

A new testing procedure was proposed in [45] to estimate rock mass deformation using the GSI, based on Hoek–Brown’s empirical constants and the Mohr–Coulomb failure criterion. The available equations allowing calculations of rock mass deformation considering the GSI are summarised in Table 1.

Table 1. Established formulas for rock mass strain modulus calculations, considering GSI.

References	Formulas	Number
[41]	$E_{rm}[GPa] = (1 - D/2)\sqrt{\frac{\sigma_{ci}}{100}}10^{\frac{GSI-10}{40}}$	(20)
[41]	$E_{rm}[GPa] = (1 - D/2)10^{\frac{GSI-10}{40}}$	(21)
[46]	$E_{rm}[GPa] = 0.1451e^{(0.0654GSI)}$	(22)
[36]	$E_{rm}[GPa] = 100\left(\frac{1-D/2}{1+e^{(75+25D-GSI)/11}}\right)$	(23)
[36]	$E_{rm}[GPa] = E\left(0.02 + \frac{1-D/2}{1+e^{(60+15D-GSI)/11}}\right)$	(24)

Based on the listed equations in Table 1, the authors adopted Formula (24) to estimate the rock mass strain modulus, as proposed by [36].

Combining Equation (6) and Formula (24) we obtain:

$$E_t = E\left[0.02 + \frac{1 - D/2}{1 + e^{((60+15D-GSI)/11)}}\right] \tag{25}$$

Currently, to characterise rock masses, rock mass classification systems can be divided into two main groups, qualitative and quantitative. The qualitative classification comprises the GSI (geological strength index); rock load; and SIA 199, while the Q; RMR; RSR; and RQD systems are quantitative in their nature [3,34,36,46,47].

Since the first rock mass classification was proposed, together with a new experimental approach to tunnel design, the system has been adopted and enhanced and now comprises a huge number of challenging factors to establish parameters [35–37,48–50]. Rock mass classification schemes are used to support the design of underground supporting structures such as RMR, Q and GSI. Some well-known classification systems are listed in Table 2.

Table 2. Rock mass classification systems (modified after [3]).

Rock Mass Classification System	Reference	Application Areas
Rock Load	[29]	Tunnels with steel support
Stand-up time	[1]	Tunnelling
New Austrian Tunnelling Method (NATM)	[51]	Tunnelling
Rock Quality Designation (RQD)	[34]	Core logging, tunnelling
Rock Structure Rating (RSR)	[49]	Tunnelling
Rock Mass Rating (RMR)	[36]	Tunnels, mines, (slopes, foundations)
Modified Rock Mass Rating (M-RMR)	[52]	Mining
Rock Mass Quality (Q)	[37]	Tunnels, mines, foundations
Strength-Block size	[53]	Tunnelling
Basic Geotechnical Classification	[54]	General
Rock Mass Strength (RMS)	[55]	Metal mining
Unified Rock Mass Classification System (URCS)	[56]	General
Communication Weakening Coefficient System (WCS)	[57]	Coal mining
Rock Mass Index (RMI)	[58]	Tunnelling
Geological Strength Index (GSI)	[38]	All underground excavations

Vásárhelyi and Kovács [58] established the experimental relationships for rock mass mechanical parameters such as compression strength, and strain modulus, which increase exponentially along with an increase in rock mass quality.

In accordance with [59], a database of GSI was proposed, where values of the GSI were adopted from the range of 13 to 80. In addition, according to [43], the value of D was equal to 0.5, corresponding to the blasting method of tunnel excavation.

3. Results and Discussion

The mechanical model for tunnel excavation used in this study was as follows: considering a tunnel of circular cross-section with a radius of R and of infinite length, a tunnel at infinite depth in an isotropic homogeneous rock mass was excavated. The tunnel was subjected to a uniform hydrostatic stress (σ_o). The uniform pressure p_o of support structures was applied to the tunnel wall surface. The field stress can be considered to be axisymmetric and all stress components at a point in the coordinate system are shown in Figure 5.

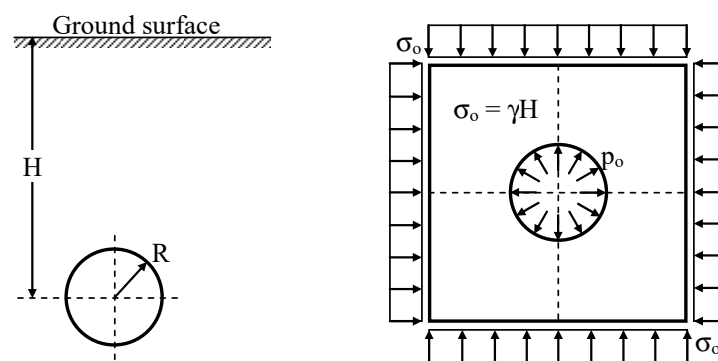


Figure 5. Mechanical model for tunnel excavation, adopted in this study.

Replacing strain modulus E in Equation (1) with the new form of E in Equation (25), the obtained formula is as follows:

$$L^* t^{*(1-\alpha)} = \frac{4 \left\{ E \left[0.02 + \frac{1-D/2}{1+e^{((60+15D-GSI)/11)}} \right] \right\} (1-\alpha)}{3\gamma H \delta} u_l^* \tag{26}$$

In fact, in relation to tunnel excavation, it is possible to determine tunnel wall surface displacement using sensors. Therefore, the authors suggest considering the values of allowable displacement for tunnel walls as a criterion for estimating tunnel stability (rock mass stability) during excavation. Values of allowable displacement for different types of rock, such as those proposed in SniP-II-94-80 in 1980, are presented in Table 3.

Table 3. Stability of rock categories regarding maximum rock material displacements (u).

Stability Category y	Rock Stability Assessment	Maximum Displacement u (mm)		
		Sedimentary Rocks (Sandstone, Siltstone, Mudstone, Limestone, Coal, etc.)	Igneous Rocks (Granite, Diorite, Porphyrite, etc.)	Rock Salts (Rock Salt, Sylvinite, Karnalite, etc.)
I	Stable	50	20	200
II	Moderate stable	50–200	20–100	200–300
III	Very unstable	200–500	100–200	300–500
IV	Highly unstable	>500	>200	>500

3.1. Numerical Modelling Analyses

To justify the use of the rheological behaviours of rocks theory in the present study, a comparison of two case studies was performed. The first one concerned comparing the experimental results of rock beams to those gained from the analytical method, and modelling using a FEM approach reflecting the potential insitu conditions simulating the scenario considered for empirical analyses. The second one was to analyse the total time-dependent vertical displacements of circular tunnel walls subjected to hydrostatic insitu stress, using Equation (25) for both analytical and FEM approaches. The first case considered rock beams with a rectangular cross section of 20×20 mm and a length of 160 mm, subjected to various values of concentrated load applied to the centre points of the beams so that the values of generated tensile stress were equal to 1.8; 2.25; and 2.7 MPa, respectively. The modulus of elasticity of rock was 14,700 MPa. Tests of simply supported rock beams were simulated using the finite element analysis using MIDAS GTS NX V.1.1 software. Based on the obtained results it was noted that the values of the instantaneous deflection y_0 were different, corresponding to the various values of subjected tensile stress. However, thanks to the homogeneity of the materials for all tests, the creep function remained constant, as shown in (19). The comparison of the deflection of rock beams achieved from experiments [3], to those attained using Equation (19) and finite element analysis, is presented in Figure 6. The figure shows good agreement between all the approaches used in the study; the best match is observed for the analytical and modelling method. The biggest discrepancies could be observed for samples tested at 1.8 MPa tensile stress. This is observed especially for an experimental approach that could be referred to as extended boundary conditions applied in the computational mode, due to the nature of expanded boundaries of FEM modelling.

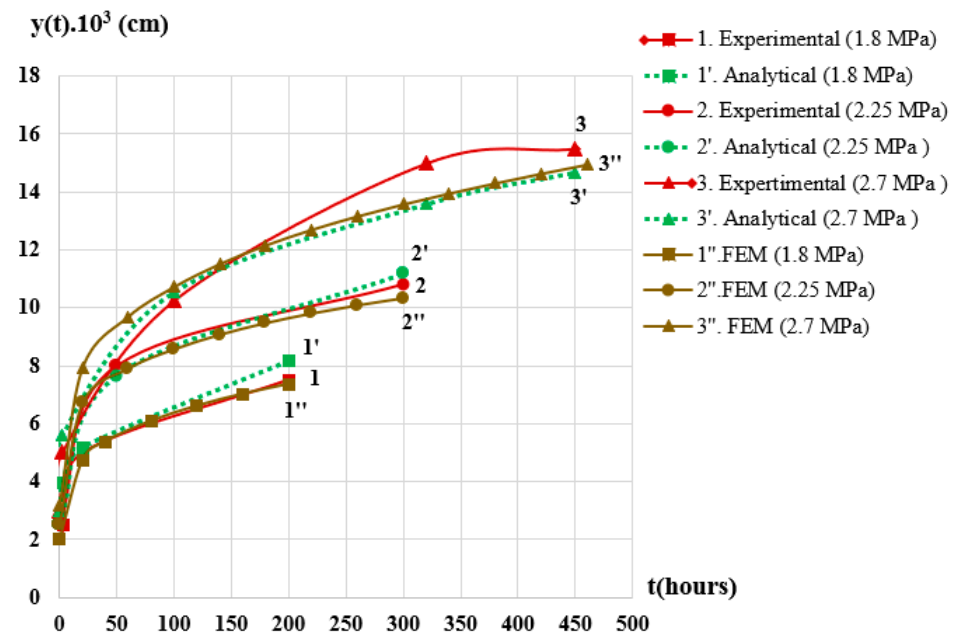


Figure 6. Comparison of results on rectangular beam deflection in time, subjected to different ranges of tensile stress, obtained via three investigation approaches (experimental, analytical and FEM).

Selected results of the FEM analyses of rock beam deflections for different testing times are shown in Figure 7.

The second case considered a circular tunnel with a radius of 3.5 m at a depth of 200 m. The parameters fed into the modeling were as follows:

- The hydrostatic in situ stress field took the value of 5.2 MPa;
- T = The modulus of elasticity E_t of the rock mass obeyed the law shown in Equation (23) with the E of 15.2 GPa;

- Values of the GSI were equal to 40, 50, and 60, respectively.

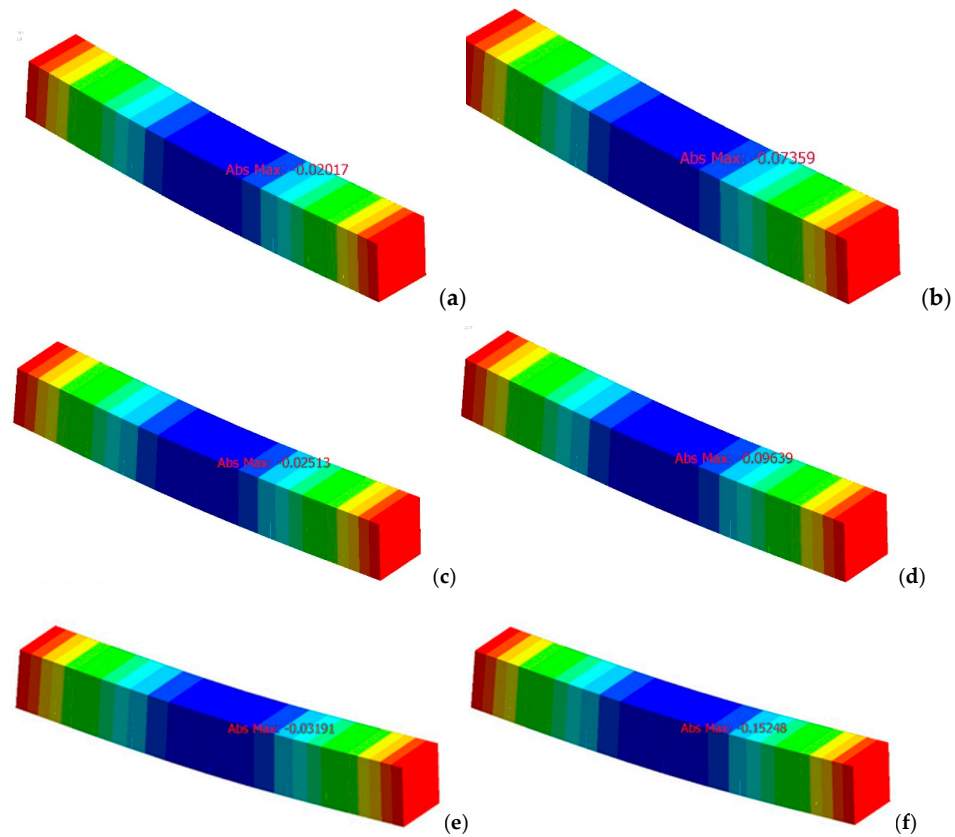


Figure 7. Beam deflection subjected to tensile stress of (a) 1.8 MP, immediate reaction; (b) 1.8 MPa, deflection after 200 h; (c) 2.25 MPa, immediate reaction; (d) 2.25 MPa, deflection after 300 h; (e) 2.7 MPa, immediate reaction; (f) 2.7 MPa, after 500 h. (where red color represent max. deflection and blue represents min. deflection).

The vertical displacement formula of a circular tunnel, in this case, was calculated according to [3], taking into account the GSI, based on Hoek–Brown’s empirical constants and Mohr–Coulomb failure criterion, as expressed in (26). The adopted formula for vertical displacements was as follows:

$$u = \frac{\gamma HR(1 + \nu)}{E \left[0.02 + \frac{1-D/2}{1+e^{((60+15D-GSI)/11)}} \right]} \left[1 + \frac{3}{2(1 + \nu)} \frac{\delta}{(1 - \alpha)} t^{1-\alpha} \right] \quad (27)$$

Comparative results obtained from Equation (27) and the FEM approach are represented in Figure 8. The results reveal that the best agreement between the approaches was observed for the highest values of GSI (60) which was due to the increased stress resistance of tested material.

Selected results of the vertical time-dependent displacement of the tunnel wall over different periods at 40, 50, and 60 GSI levels are shown in Figure 9. Analyses of the modelling results revealed that tunnel wall vertical displacement obtained using the FEM approach gave close values to those calculated using Formula (27). The comparative results are in good agreement with those obtained by [1,3,5,6]. Thereby, the effect of the GSI on stand-up time calculation is convincing. This allows for the optimisation of supporting structure design in tunnelling and provides an opportunity to avoid potential risks and hazards during tunnel excavation works.

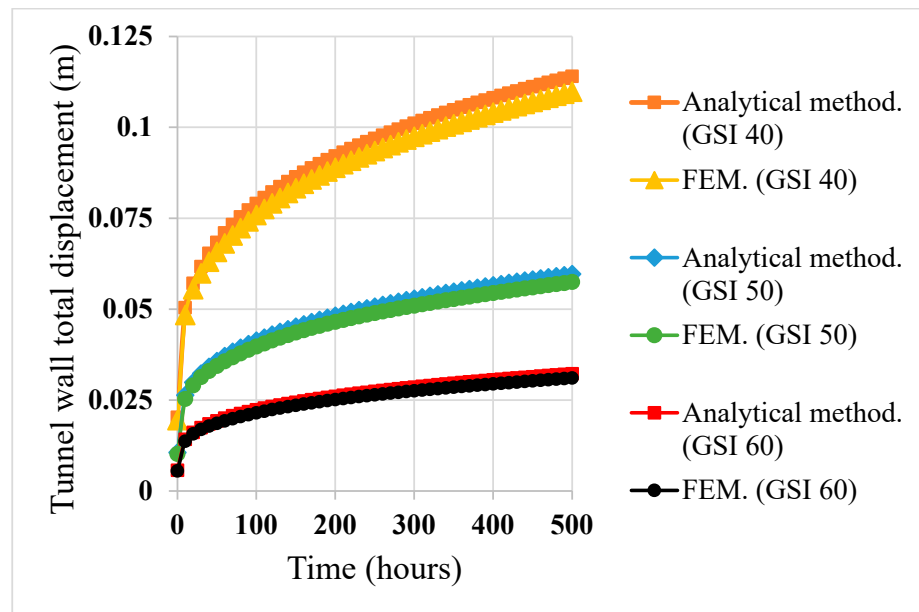


Figure 8. Total time-dependent displacement curves of tunnel walls gained using analytical and finite element methods according to various values of GSI (40, 50, 60).

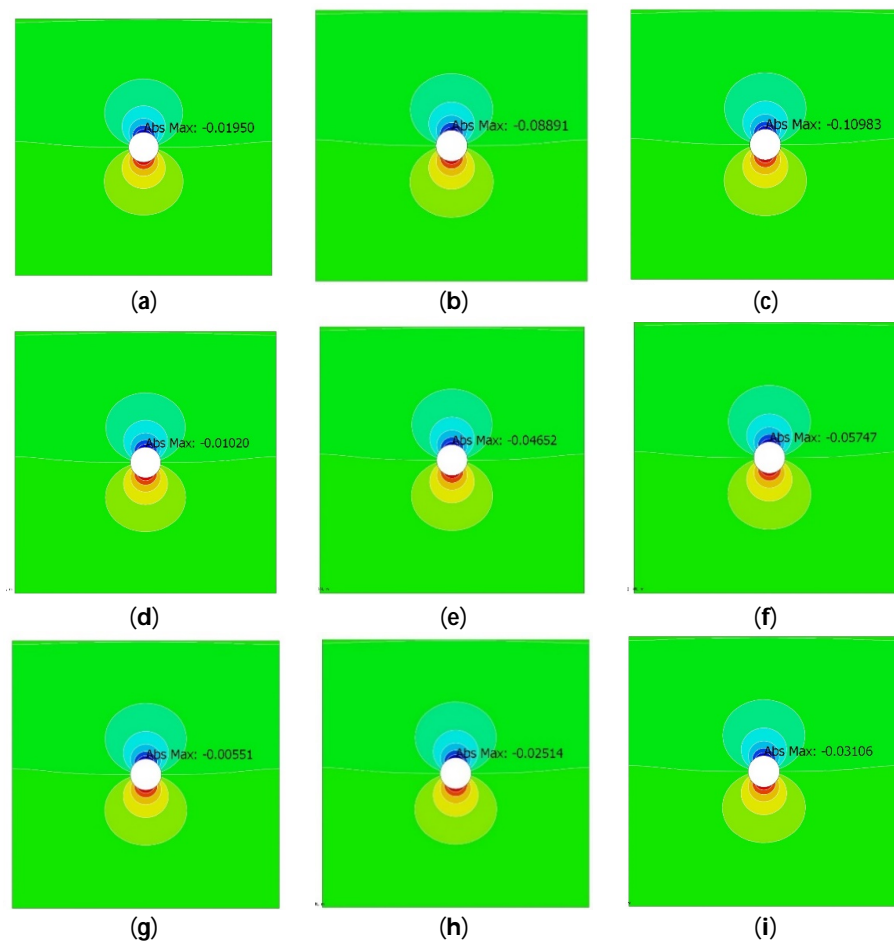


Figure 9. Vertical displacements of tunnel wall (a) at GSI 40, immediate reaction; (b) at GSI 40, after 200 h; (c) at GSI 40, after 500 h; (d) at GSI 50, immediate reaction; (e) at GSI 50, after 200 h; (f) at GSI 50, after 500 h; (g) at GSI 60, immediate reaction; (h) at GSI 60, after 200 h; and (i) at GSI 60, after 500 h. (heat map presents the displacement distribution).

3.2. GSI Influencing Stand-Up Time Parametric Analyses

To perform the analyses of the influence of GSI on stand-up time for an unsupported tunnel span, the authors considered a set of input data as the allowable displacement according to table $5u_l^* = 50 \text{ mm}$; rock mass unit weight $\gamma = 26 \text{ kN/m}^3$; strain modulus $E = 29.5 \text{ GPa}$; Poisson's ratio $\nu = 0.3$; and tunnel depth $H = 200 \text{ m}$. Young's modulus and Poisson's ratio are listed in Table 4. It was observed that the highest settlements are at the immediate response stage. Figure 10 indicates the relationship between the stand-up time of the unsupported tunnel span and of the GSI; the values are equal to 5, 10, 20, 40, 60, 80, and 100, respectively. In Figure 10 it is revealed that the increase in the GSI results in an increase in stand-up time. This trend shows a good agreement with [33].

Table 4. General properties of material.

Rock Type	Young's Modulus E, (GPa)	Poisson's Ratio ν
Aleurolite (siltstone)	6.2	0.07 ÷ 0.40
	14.0	0.28 ÷ 0.37
	23.5	0.18 ÷ 0.32

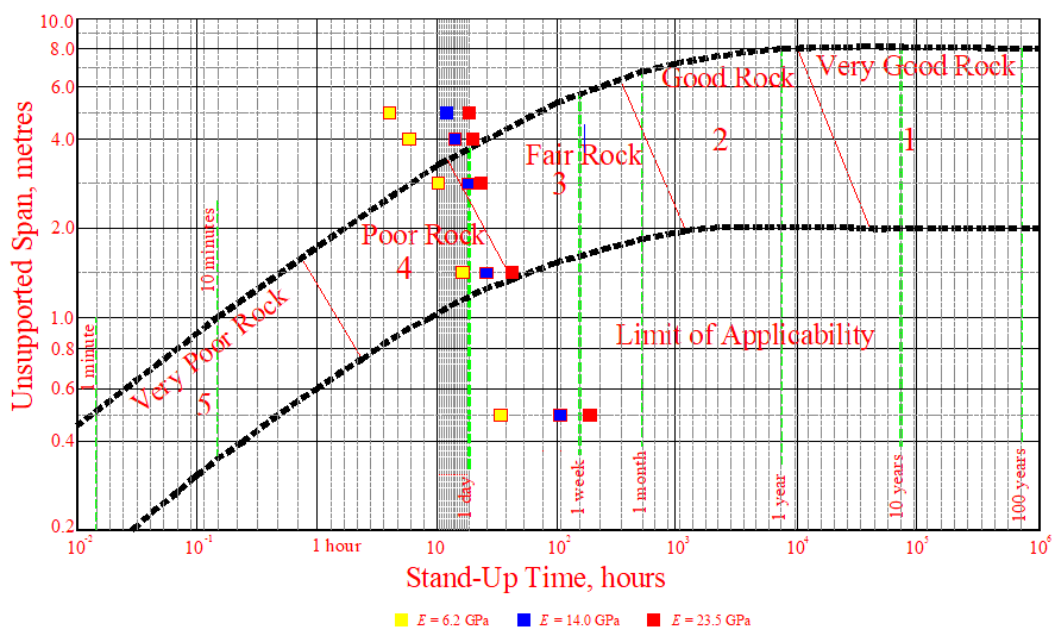


Figure 10. Various values of stand-up time correspond to different qualities of rock using Young's modulus.

Similar to the previous analyses, the graphs presented in Figure 11 reveal that the lower the values of rock using Young's modulus, the less the values of the stand-up time of the unsupported tunnel became. The achieved results are in good agreement with [5] and [3].

3.3. Influence of Maximum Allowable Displacement Analyses

To clarify the effect of allowable displacement on stand-up time, argillite stone was analysed with a set of input data expressed as Young's modulus $E = 15.2 \text{ GPa}$; Poisson's ratio $\nu = 0.3$; GSI = 40; and tunnel depth $H = 200 \text{ m}$. Values of allowable displacement varied in a range from 20 mm to 100 mm with a step of 20 mm. Figure 11 confirms the effect of the allowable displacement of tunnel walls on stand-up time. Accordingly, the increase in the values of the allowable displacement of tunnel walls results in the increase

of stand-up time of unsupported tunnel spans. Thus, the values of allowable displacement strongly depend on the types of rock material surrounding the tunnel. To sum up, the findings are in agreement with those published in [3].

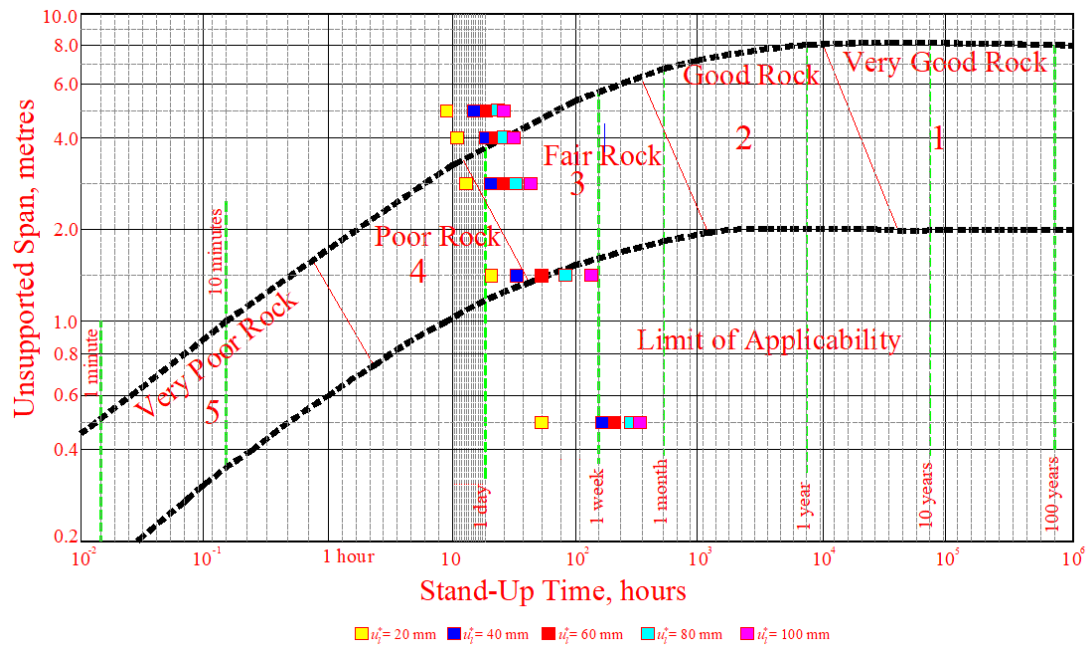


Figure 11. Relationship of unsupported tunnel span with stand-up time corresponding to various values of allowable displacement of tunnel.

4. Conclusions

The stand-up time of the rock mass around an unsupported tunnel plays a crucial role in underground construction in general, and tunnelling in particular. The estimation of the values of stand-up time significantly affects the decision-making procedures of choosing effective excavation methods as well as the supporting systems. In the present paper, the authors conducted experimental and theoretical studies on the effect of stand-up time for rock masses around the tunnel on an unsupported span, based on mechanical parameters of rock such as the strain modulus, and the geological strength index (GSI). The analyses took into account values of allowable displacement, as well as hereditary creep properties.

Using the two approaches of analysing the results for scrutinising the overall time-dependent vertical displacements of circular tunnel walls under the influence of hydrostatic in situ stress using empirical and FEM methods, it was revealed that the effect of the GSI on stand-up time calculation is reliable and allows optimisation of supporting structure design in tunnelling, to avoid potential risks and hazards during tunnel excavation works.

The research on how the permissible displacement influences the stand-up time of argillite stone, utilising a specified set of input data validates the influence of permissible displacement of tunnel walls. Consequently, an increase in the allowable displacements of tunnel walls leads to an enhancement in the stand-up time of an unsupported tunnel span. Clearly, the permissible displacement values are significantly influenced by the types of rock materials surrounding the tunnel. As a result, the authors highlight the matching relationships established using Lauffer’s methods for rock mass; Young’s modulus; GSI; tunnel depth; and values of allowable displacement to stand-up time of an unsupported tunnel. The results also confirm the findings obtained using Bieniawski’s method, as well as enhance the study results obtained by [3], by taking into consideration time factors in the calculation of rock mass stand-up time.

A noteworthy advancement in the present study is the incorporation of hereditary creep properties into the calculations. This temporal consideration adds a dynamic dimension to the estimation of stand-up time, addressing a crucial aspect that has usually been

neglected in previous research. By acknowledging the time factor, the authors bring a more realistic perspective to the assessment of rock mass stability, thereby contributing to the refinement of existing models.

In conclusion, the authors' work not only reaffirms established correlations, but also pioneers the integration of time-dependent factors, providing a more accurate understanding of the stand-up time for rock masses around unsupported tunnels. The present research contributes significantly to the optimisation of underground construction practices, offering a valuable resource for engineers and practitioners in the scientific field of underground construction.

Author Contributions: Conceptualisation, P.D.N., H.H.N. and M.V.N.; methodology, P.D.N. and H.H.N.; software, P.D.N., H.H.N. and H.H.D.; validation, M.V.N. and H.H.D.; formal analysis, E.K., P.D.N., P.O. and H.H.N.; investigation, H.H.D. and H.H.N.; resources, P.D.N.; data curation, H.H.D. and H.H.N.; writing—original draft preparation, P.D.N., P.O. and E.K.; writing—P.O. and E.K.; visualisation, H.H.N., P.O. and E.K.; supervision, M.V.N., P.D.N. and E.K.; project administration, P.D.N. and H.H.N.; funding acquisition, P.D.N., E.K. and P.O. All authors have read and agreed to the published version of the manuscript.

Funding: This research was funded by the Vietnamese Ministry of Education and Training under Grant No. B2022-MDA-07.

Institutional Review Board Statement: Not applicable.

Informed Consent Statement: Not applicable.

Data Availability Statement: Data are contained within the article.

Acknowledgments: The authors gratefully acknowledge the financial support provided by the Vietnamese Ministry of Education and Training under Grant No. B2022-MDA-07.

Conflicts of Interest: The authors declare no conflicts of interest.

Abbreviations

List of symbols:

L^*	unsupported tunnel span [m]
t^*	stand up time [h]
α	dimensionless empirical parameter
δ	dimensional parameter (s)
E	modulus of elasticity of the rock mass [MPa]
γ	the unit weight of the rock mass
H	tunnel depth [m]
u_i^*	allowable displacement for sustainable condition of sedimentary rocks [m]
GSI	Geological Strength Index
RQD	degree of jointing (Rock Quality Designation)
$\varepsilon(t)$	strain at moment t [mm/mm]
$\sigma(t)$	stress at moment t , [MPa]
τ	time before instant t [h]
$L(t, \tau)$	creep kernel function characterising the strain rate.
Φ	creep function
σ_0	tensile stress due to bending moment, MPa
M	The maximum bending moment at the centre beam cross section [kNm]
h	beam height [m]
ν	Poisson's ratio

References

1. Lauffer, H. Gebirgsklassifizierung für den Stollenbau. *Geol. Bauwes.* **1958**, *24*, 46–51.
2. Hooke, R. *Lectures De Potentia Restitutiva, or of Spring Explaining the Power of Springing Bodies*; Martyn, J., Ed.; Royal Society: London, UK, 1678.
3. Nguyen, V.M.; Nguyen, Q.P. Analytical solution for estimating the stand-up time of the rock mass surrounding tunnel. *Tunn. Undergr. Space Technol.* **2015**, *47*, 10–15. [[CrossRef](#)]
4. Bieniawski, Z.T. Classification of Rock Masses for Engineering: The RMR System and Future Trends. In *Chapter 22 in Comprehensive Rock Engineering*; Elsevier: Amsterdam, The Netherlands, 1993; pp. 553–573.
5. Myer, L.R.; Brekke, T.L.; Korbin, G.E.; Kavazanjian, E.; Mitchell, J.K. *Stand-Up Time of Tunnels in Squeezing Ground; Part i. A Physical Model Study*. DOT-TST-77/59 Final Rpt.; Department of Transportation: Washington, DC, USA, 1977.
6. Damjanac, B.; Fairhurst, C. Evidence for a long-term strength threshold in crystalline rock. *Rock Mech. Rock Eng.* **2010**, *43*, 513–531. [[CrossRef](#)]
7. Eberhardt, E.; Stimpson, B.; Stead, D. The influence of mineralogy on the initiation of microfractures in Granite. In Proceedings of the 9th International Congress on Rock Mechanics, Paris, France, 25–28 August 1999; A.A. Balkema: Rotterdam, The Netherlands, 1999; pp. 1007–1010.
8. Fabre, G.; Frédéric, P. Creep and time-dependent damage in argillaceous rocks. *Int. J. Rock Mech. Min. Sci.* **2006**, *43*, 950–960. [[CrossRef](#)]
9. Song, F.; Rodriguez-Do, A.; Olivella, S.; Zhong, Z. Analysis and modelling of longitudinal deformation profiles of tunnels excavated in strain-softening time-dependent rock masses. *Comput. Geotech.* **2020**, *125*, 103643. [[CrossRef](#)]
10. Aleja, L.R.; Rodríguez-Do, A.; Veiga, M. Plastic radii and longitudinal deformation profiles of tunnels excavated in strain-softening rock masses. *Tunn. Undergr. Space Technol.* **2012**, *30*, 169–182. [[CrossRef](#)]
11. Arzúa, J.; Aleja, L.R. Dilation in granite during servo-controlled triaxial strength tests. *Int. J. Rock Mech. Min. Sci.* **2013**, *61*, 43–56. [[CrossRef](#)]
12. Song, F.; Rodriguez-Do, A. Numerical solutions for tunnels excavated in strain-softening rock masses considering a combined support system. *Appl. Math. Model.* **2021**, *92*, 905–930. [[CrossRef](#)]
13. Paraskevopoulou, C. Time-Dependency of Rocks and Implications Associated with Tunnelling. Ph.D. Thesis, Queen's University, Kingston, ON, Canada, 2016.
14. Paraskevopoulou, C.; Diederichs, M. Analysis of time-dependent deformation in tunnels using the Convergence-Confinement Method. *Tunn. Undergr. Space Technol.* **2018**, *71*, 62–80. [[CrossRef](#)]
15. Song, F.; Wang, H.; Jiang, M. Analytically-based simplified formulas for circular tunnels with two liners in viscoelastic rock under anisotropic initial stresses. *Constr. Build. Mater.* **2018**, *175*, 746–767. [[CrossRef](#)]
16. Song, F.; Wang, H.; Jiang, M. Analytical solutions for lined circular tunnels in viscoelastic rock considering various interface conditions. *Appl. Math. Model.* **2018**, *55*, 109–130. [[CrossRef](#)]
17. Chu, Z.; Wu, Z.; Liu, B.; Liu, Q. Coupled analytical solutions for deep-buried circular lined tunnels considering tunnel face advancement and soft rock rheology effects. *Tunn. Undergr. Space Technol.* **2019**, *94*, 103111. [[CrossRef](#)]
18. Sulem, J.; Panet, M.; Guet, A. An analytical solution for time-dependent displacements in a circular tunnel. *Int. J. Rock Mech. Min. Sci. Geomech. Abstr.* **1987**, *24*, 155–164. [[CrossRef](#)]
19. Sterpi, D.; Giancarlo, G. Visco-plastic behaviour around advancing tunnels in squeezing rock. *Rock Mech. Rock Eng.* **2009**, *42*, 319–339. [[CrossRef](#)]
20. Bobrowsky, P.T.; Marker, B. (Eds.) *Encyclopedia of Engineering Geology*; Springer: Berlin/Heidelberg, Germany, 2018.
21. Griggs, D. Creep of rocks. *J. Geol.* **1939**, *47*, 225–251. [[CrossRef](#)]
22. Le Comte, P. Creep in rock salt. *J. Geol.* **1965**, *73*, 469–484. [[CrossRef](#)]
23. Langer, M. The rheological behaviour of rock salt. In Proceedings of the 1st Conference on Mechanical Behaviour of Salt, University Park, PA, USA, 9–11 November 1984; Trans Tech Publications Ltd.: Clausthal, Germany, 1984; pp. 201–230.
24. Andargoli, E.; Shahriar, K.; Ramezanzadeh, A.; Goshtasbi, K. Presenting an experimental creep model for rock salt. *J. Min. Environ.* **2018**, *9*, 441–456.
25. Paraskevopoulou, C.; Perras, M.; Diederichs, M.; Amann, F.; Löw, S.; Lam, T.; Jensen, M. The three stages of stress relaxation—Observations for the time-dependent behaviour of brittle rocks based on laboratory testing. *Eng. Geol.* **2017**, *216*, 56–75. [[CrossRef](#)]
26. Barla, G.; Borgna, S. Tunnelling in squeezing rock conditions. In Proceedings of the ROCKSITE-99, Bangalore, India, 6–9 December 1999; pp. 97–108.
27. Zheng, X.; Wu, K.; Shao, Z.; Yuan, B.; Zhao, N. Tunnel Squeezing Deformation Control and the Use of Yielding Elements in Shotcrete Linings A Review. *Material* **2022**, *15*, 391. [[CrossRef](#)]
28. Terzaghi, K. *Rock Defects and Loads on Tunnel Supports*; Harvard University: Cambridge, MA, USA, 1946.
29. Volterra, V. *Theory of Functionals and of Integro-Differential Equations*; Blackie: London, UK, 1931.
30. Bulychev, N.S. *Mechanics of Underground Structures*; Nedra: Moscow, Russia, 1982.
31. Pasik, T.; Chalecki, M.; Koda, E. Analysis of embedded retaining wall using the subgrade reaction method. *Stud. Geotech. Mech.* **2015**, *37*, 59–73. [[CrossRef](#)]
32. Hoek, E.; Diederichs, M.S. Empirical estimation of rock mass modulus. *Int. J. Rock Mech. Min. Sci.* **2006**, *43*, 203–215. [[CrossRef](#)]

33. Kawalec, J.; Grygierek, M.; Koda, E.; Osinski, P. Lessons learned on geosynthetics applications in road structures in Silesia mining region in Poland. *Appl. Sci.* **2019**, *9*, 1122. [[CrossRef](#)]
34. Bieniawski, Z.T. Engineering classification of jointed rock masses. *Civ. Eng. S. Afr.* **1973**, *15*, 335–344.
35. Barton, N.R.; Bieniawski, Z.T. *RMR and Q-Setting Records Straight*; Tunnels & Tunnelling International; Progressive Media Markets Ltd.: London, UK, 2008; pp. 26–29.
36. Barton, N.; Lien, R.; Lunde, J.J.R.M. Engineering classification of rock masses for the design of tunnel support. *Rock Mech.* **1974**, *6*, 189–236. [[CrossRef](#)]
37. Hoek, E.; Brown, E.T. Practical estimates of rock mass strength. *Int. J. Rock Mech. Min. Sci.* **1997**, *34*, 1165–1186. [[CrossRef](#)]
38. Zhang, C.Q.; Yu, J.; Chen, J.; Lu, J.J.; Zhou, H. Evaluation method for potential rockburst in underground engineering. *Rock Soil Mech.* **2016**, *37*, 341–349.
39. Hoek, E. Strength of rock and rock masses. *ISRM News J.* **1994**, *2*, 4–16.
40. Hoek, E.; Carranza-Torres, C.; Corkum, B. Hoek-Brown failure criterion-2002 edition. *Proc. NARMS-Tac* **2002**, *1*, 267–273.
41. Cai, M.; Kaiser, P.K.; Tasaka, Y.; Maejima, T.; Morioka, H.; Minami, M. Generalized crack initiation and crack damage stress thresholds of brittle rock masses near underground excavations. *Int. J. Rock Mech. Min. Sci.* **2004**, *41*, 833–847. [[CrossRef](#)]
42. Sonmez, H.; Ulusay, R. Modifications to the geological strength index GSI and their applicability to stability of slopes. *Int. J. Rock Mech. Min. Sci.* **1999**, *36*, 743–760. [[CrossRef](#)]
43. Singh, B.; Goel, R.K. *Engineering Rock Mass Classification*; Elsevier: Amsterdam, The Netherlands, 1999.
44. Lee, Y.-L.; Ma, C.-H.; Lee, C.-M. Analytical Solution Implemented by an Incremental Procedure for the Ground Reaction Based on Hoek–Brown Failure Criterion in the Tunnel Convergence-Confinement Method. *Civ. Eng.* **2023**. *in print*.
45. Gokceoglu, C.; Sonmez, H.; Kayabasi, A. Predicting the deformation moduli of rock masses. *Int. J. Rock Mech. Min. Sci.* **2003**, *40*, 701–710. [[CrossRef](#)]
46. Deere, D.U.; Hendron, A.J.; Patton, F.D.; Cording, E.J. Design of surface and near-surface construction in rock. In Proceedings of the ARMA US Rock Mechanics/Geomechanics Symposium, Minneapolis, MN, USA, 25–28 September 1966; p. ARMA-66.
47. Qazi, A.; Singh, K. Rock Mass Classification Techniques and Parameters a Review. *J. Min. Environ.* **2023**, *14*, 155–178.
48. Wickham, G.E.; Tiedemann, H.R.; JACOBS ASSOCIATES INC SAN FRANCISCO CA. Research in Ground Support and Its Evaluation for Coordination with System Analysis in Rapid Excavation. *Contract Rep. H* **1972**, *2*, 210038.
49. Kundu, J.; Sarkar, K.; Singh, A.K.; Singh, T.N. Continuous functions and a computer application for Rock Mass Rating. *Int. J. Rock Mech. Min. Sci.* **2020**, *129*, 104280. [[CrossRef](#)]
50. Aygar, E.B. Performance of the Flexible and Rigid Lining under Earthquake Impact and Weakness of the New Austrian Tunneling Method NATM Principles, a Specific Case Study of the Bolu Tunnel. *Sustainability* **2023**, *15*, 15544. [[CrossRef](#)]
51. Özkan, İ. Modified Rock Mass Rating M-RMR System and Roof Behavior Model. Ph.D. Thesis, Middle East Technical University, Ankara, Turkey, 1995.
52. Franklin, J.A. Safety and economy in tunneling. In Proceedings of the 10th Canadian Rock Mechanics Symposium, Kingston, ON, Canada, 2–4 September 1975; Volume 1, pp. 27–53.
53. Bieniawski, Z.T.; Hawkes, I. International society for rock mechanics commission on standardization of laboratory and field tests Suggested methods for the quantitative description of discontinuities in rock masses. *J. Rock Mech. Min. Sci.* **1978**, *15*, 319–368.
54. Stille, H.; Groth, T.; Fredriksson, A. FEM-analysis of Rock Mechanical Problems with JOBFEM. *Stiftelsen Bergteknisk Forsk.–BeFo Stockh.* **1982**, *307*, 82.
55. Williamson, D.A. Unified rock classification system. *Bull. Assoc. Eng. Geol.* **1984**, *21*, 345–354. [[CrossRef](#)]
56. Singh, R.N.; Elmherig, A.M.; Sunu, M.Z. Application of rock mass characterization to the stability assessment and blast design in hard rock surface mining excavations. In Proceedings of the ARMA US Rock Mechanics/Geomechanics Symposium, Tuscaloosa, AL, USA, 28–30 June 1986; p. ARMA-86.
57. Palmström, A.; Strömme, B. The Rock Mass index RMD applied in rock mechanics and rock engineering. *J. Rock Mech. Tunn.* **1996**, *11*, 1–40.
58. Vásárhelyi, B.; Kovács, D. Empirical methods of calculating the mechanical parameters of the rock mass. *Period. Polytech. Civ. Eng.* **2017**, *61*, 39–50. [[CrossRef](#)]
59. Polemis Júnior, K.; Silva Filho, F.C.D.; Lima-Filho, F.P. Estimating the rock mass deformation modulus A comparative study of empirical methods based on 48 rock mass scenarios. *REM Int. Eng. J.* **2021**, *74*, 39–49. [[CrossRef](#)]

Disclaimer/Publisher’s Note: The statements, opinions and data contained in all publications are solely those of the individual author(s) and contributor(s) and not of MDPI and/or the editor(s). MDPI and/or the editor(s) disclaim responsibility for any injury to people or property resulting from any ideas, methods, instructions or products referred to in the content.